

Reliability Analysis of Francis Turbine Cracking Using Gamma Frailty Model and Censored Historical Maintenance Data

Théophile Mbuyi Tshibangu¹, Guyh Dituba Ngoma¹, Martin Gagnon² and Sébastien Carle³

¹*School of Engineering, University of Quebec in Abitibi-Témiscamingue, 445 Boulevard de l'Université, Rouyn-Noranda, J9X 5E4, Canada*

²*Hydro-Québec's Research Institute, 1800, boulevard Lionel-Boulet, Varennes, Quebec, J3X 1S1, Canada*

³*Hydro-Québec, 1095 Rue Saguenay, Rouyn-Noranda, Quebec, J9X 5B5, Canada*

Keywords: Gamma Frailty Model, Reliability, Cracks, Hydraulic Turbine, Censored Historical Data.

Abstract: All over the world, the need for electrical energy has increased dramatically, forcing hydroelectric power plants to operate under non-standard conditions. This leads to premature fatigue cracking and consequently to multiple crack inspections. In this research, a probabilistic model is developed based on frailty and censoring. The model takes advantage of the use of a Non-Homogeneous Poisson Process (NHPP) because turbine runners are considered as repairable parts. We develop the marginal likelihood expression incorporating frailty effect using gamma frailty distribution and we use the stochastic gradient descent (SGD) algorithm to obtain the optimal parameters. Furthermore, instead of considering the frailty effect z as a random variable, we decide to derive its expression from the individual unconditional likelihood function that has been also optimized. Finally, we compare reliability and cumulative hazard functions between family members. We then confirm the results obtained by comparing reliability between two families that behaved differently. Results show that frailty effect, that is function of failure statuses and individual final time of observation for a specific component has played an important role in differentiating heterogeneity among groups of the same family. Reliability curves clearly demonstrate heterogeneity within and between families.

1 INTRODUCTION

Industrial development throughout the world and even daily life of human beings have become largely dependent on electrical energy. Among electricity production methods, hydropower represents less than 20% of global production (Liu et al., 2016a; Trivedi and Cervantes, 2017). However, it far exceeds other forms of green energy production combined. The availability of turbine runner and alternator units is therefore essential, especially in region such as Quebec with limited potentials in other forms of renewable energy. Hydro-Québec, the electricity production company in Canada, with a fleet of 60 hydroelectric power plants, saw a drop in electricity sales from 216.2 TWh in 2022 to 200.3 TWh in 2023 (Hydro-Québec, 2023). Cavitation and cracks that appear on some turbine runners families, limit the availability of the units and consequently increase maintenance costs, as well as the number of shutdowns and start-ups due to systematic inspections and repairs. However, these transient zones of start-ups and

shutdowns are generally responsible of turbine cracking because of high stress fluctuations (Morin et al., 2021). On the other hands, some families are run in off-design conditions to maintain the demand in electrical energy (Morin et al., 2021).

Basically, a turbine runner is designed to withstand fatigue damage. Unfortunately, fatigue cracks appear as a random effects (Georgievskaja, 2020) in some turbine runners families. Researchers have been scrambling to identify the principal causes of these cracks (Liu et al., 2016b) as indicated in Figure 1. Analytical, physical, numerical and data based models were developed. For example, (Morin et al., 2021) analysed the transients effects on the lifespan of turbine runner. They concluded that the startup, shutdown and time of speed no load create fluctuations that lead probably to cracks. (Gagnon et al., 2010) evaluated the fluctuations of the stresses at the startup in order to optimize the life expectancy of a turbine runner. (Thibault et al., 2015) examined the material properties especially 13% Cr-4%Ni stainless. Furthermore, site experiments and campaign mea-

measurements have been used to evaluate reliability (Trivedi et al., 2013). For instance, (Gagnon et al., 2014) made strain measurement and used operation history to capture reliability of turbine runners. (Bajgholi et al., 2021) evaluated the use of advanced ultrasonic inspection to learn about the manufacturing flaws and cracks. (Bajgholi et al., 2023) evaluated reliability by using a non destructive testing to capture manufacturing flaws. In addition, (Wang et al., 2012), (Zhang et al., 2019) discovered that the manufacturing flaws in runner blades such as heterogeneity, anisotropic character and thinning of blade thicknesses could be the cause of cracking when runner is working under critical conditions.

These studies have been done based on simplified physical models simulations or standard measurements. However, finding a model that incorporates the complexity of all the predominant causes would be a major challenge, as the various causes cannot be combined in a physical model (residual stresses, transient conditions, manufacturing flaws, etc.) (Xiao et al., 2010, Xiao et al., 2008). In addition, experimental measurements have given results quite different with what were really observed in hydroelectric plant.

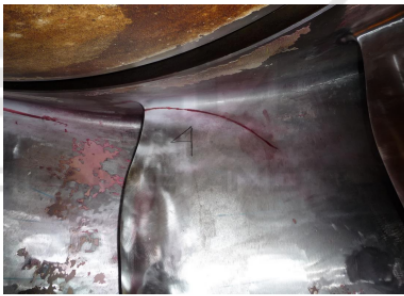


Figure 1: Cracks on Francis runner blades.

Another approach is the use of probabilistic model based on operational hydroelectric site data to apprehend crack initiation (Gagnon et al., 2014). For instance, (Georgievskaja, 2021) run an algorithm using operational data to predict the remaining lifetime for turbine runners that were above 30 years old. These measurement processes are essentially costly when it comes to monitoring each individual turbine runner.

The third approach is based on experience. This approach makes use of historical maintenance data to evaluate reliability of components. For example, (Ivanchenko and Prokopenko, 2020) analyzed cracks on turbine blades based on failure history. They found that residual stresses and internal defects in the material promote cracking. They predict the possible location of the crack according to maintenance data and show that reliability is decreasing with the age.

This study is also based on the processing of real historical maintenance data for two turbine families. The main objective is to develop a probabilistic model that can reflect what is actually observed in hydroelectric power plants. To do this, we build a model that incorporates the individuality of each turbine in terms of its frailty effect, and use censored maintenance data to capture the reliability information stored in preventive inspections and crack observations. By classifying individuals with similar reliability trends, we can decide whether to reduce unnecessary systematic inspections or monitor just one of the individuals of the same type with similar reliability trends. The choice of two different families will enable us to validate the robust family and the most vulnerable one observed.

2 FRAILTY MODEL

Simulations done by (Gagnon and Nicolle, 2019) demonstrate that non-uniformities and eccentricities of a turbine runner assembly could affect the dynamic behaviour among the same family. This combined with manufacturing variabilities make each turbine unique and explain the fact that cracks do not appear in the same way among the family members. Hence, turbine runners could not be considered as homogeneous in the same family. Furthermore, turbine runners that were repaired and welded will show different behaviour. All these factors demonstrate that each turbine runner is unique and has its own frailty. Frailty is an unobserved covariate or a random effect that can not be measured but affects the reliability in the model (Therneau et al., 2003).

Indeed, the behaviour of a repairable component can be captured in historical maintenance data, and can lead to a frailty parameter that distinguishes components from each other, even if they belong to the same family. One of the best methods is to optimize censored maintenance data using a survival analysis model.

2.1 Censoring

Censoring generally communicates partial information on the observation of the event. When a visual inspection is carried out and no crack (fatigue damage) is detected, this information is censored (Wienke, 2010).

Let us consider a repairable entity with observation times t_1, t_2, \dots, t_k which could be inspection or repair times, let $t_1^*, t_2^*, \dots, t_k^*$ be the survival times when failure occurs (crack detected) and c_1, c_2, \dots, c_k be the censored times (no crack detected). At each obser-

vation, we will have the couple (t_i, δ_i) (Munda et al., 2012) such that:

$$\delta_i = \begin{cases} 1 & \text{when } t_i^* \leq c_i, t_i \text{ is not censored} \\ 0 & \text{when } t_i^* > c_i, t_i \text{ is censored} \end{cases} \quad (1)$$

Each δ represents a failure status, indicating whether or not the crack was observed at the time of the event (crack inspections during cavitation repair, systematic inspections or crack detection).

2.2 Stochastic Process

There are mathematical probabilistic models that can be used to process time-dependant data to obtain a distribution. These models differ depending on whether the observation data are for a repairable entity or not (Ascher, 2008).

A non-repairable entity has a unique lifetime. It is replaced once the failure has occurred. The reliability of this type of entity can be modeled by probabilistic mathematical distributions such as Kaplan Meier, exponential distribution, Weibull's distribution (Asfaw and Lindqvist, 2015). Some repairable components can be replaced when the cost of maintenance becomes too excessive. In this case, they are considered and modeled as non-repairable components. Maintenance activities on a repairable entity can either bring it back to the state where it looks new (as good as new) by improving the reliability, or back to the state it was before the failure was observed (as bad as old) (Love and Guo, 1991),(Ascher, 1968).

Several stochastic processes exist for repairable entities (Slimacek and Lindqvist, 2016):

- Renewal Process (RP)
- Homogeneous Poisson Process (HPP)
- Nonhomogeneous Poisson Process (NHPP)
- Branching Poisson Process (BPP)

In literature, NHPP is most suitable for repairable entities in which failures occur randomly (Slimacek and Lindqvist, 2016). Therefore, the minimal repair assumption is used which means that after repair, the reliability still decreasing as if failure were not appeared. Several mathematical laws exist to model a NHPP. However, the power law remains the most practical (Oliveira et al., 2013),(Brown et al., 2023). The baseline hazard function of the power law is given in Equation 1.

$$h_0(t) = \omega \rho t^{\rho-1} \quad (2)$$

with ω the scale parameter and ρ the shape parameter of the curve.

- If $\rho > 1$, the system is deteriorating (sad system),
- If $0 < \rho < 1$, the system is improving (happy system)

If $\rho = 1$, the failure intensity function is a constant and the model can be used in a HPP process with the exponential distribution.

2.3 Frailty Distribution

In survival analysis, several models are not giving expected results for the fact that heterogeneity effect was not taken into account. Incorporating frailty in the model allows to consider both random effects and unobservable heterogeneity in the survival analysis.

Let z be a positive time-independent random factor that acts multiplicatively on the intensity function. We assume that the z is time-independent and is related to each entity. However, this factor, in general, can also vary over time depending on certain criteria or the data of the problem. The intensity function with frailty effect is:

$$h(t) = z \omega \rho t^{\rho-1} \quad (3)$$

$z > 1$ means that failure will often occur and $z < 1$ leads to less failure occurrence (Vaupel et al., 2023). In case we will find $z = 1$, this means that the components have no heterogeneity and can only be modelled by a power law without frailty effect. In addition, components with $z = 0$ fragility refer to those with higher reliability, especially when nothing is recorded to classify them.

The random variable z is expected to follow a specific probability distribution. Let $f(z)$ be the frailty probability density function of z . For time-event data, several univariate frailty models exist. The most widely used are the Gamma frailty and inverse Gaussian frailty models. However, the Gamma frailty distribution is the most popular because of the gamma function's mathematical properties and computational aspects (Asfaw and Lindqvist, 2015).

2.3.1 Gamma Frailty Distribution

(Duchateau and Janssen, 2008), (Brown et al., 2023), (Asfaw and Lindqvist, 2015) used gamma distribution to model heterogeneity. (Abbring and Berg, 2007) has revealed that in most cases, for a large class, the frailty distribution converges to a gamma distribution as time approaches infinity. As we are using data for turbine runner that approach to end of lifetime, we have considered gamma frailty distribution in the model. In the literature, the likelihood comparison of the data obtained with frailty gamma distribution gave better results compared to traditional parametric models (Brown et al., 2023). The probability density function of the gamma distribution is :

$$f(z) = \frac{1}{\Gamma(k)} \lambda^k z^{k-1} e^{-\lambda z} \quad (4)$$

with λ the inverse scale parameter and k the shape parameter. Using the Lapace transform and mathematical properties of gamma function, we can show that the mean and variance of the gamma distribution respectively are

$$\text{var}(z) = \frac{k}{\lambda^2} \quad (5)$$

and

$$E(z) = \frac{k}{\lambda}. \quad (6)$$

With z being a positive number. Let assume that the mean of the gamma distribution is unit and let call the variance by θ . Therefore $k = \frac{1}{\theta} = \lambda$. The probability density function for gamma frailty distribution becomes:

$$f(z) = \frac{1}{\Gamma(\frac{1}{\theta})} \left(\frac{1}{\theta}\right)^{\frac{1}{\theta}} z^{\frac{1}{\theta}-1} e^{-\frac{z}{\theta}} \quad (7)$$

2.3.2 Likelihood Function

One of the best way for determining different parameters of the frailty model that could highly fit with data is to optimize the likelihood function. Let j be a repairable entity with a finite number of failures n_j , with $j = 1, 2, \dots, m$ components in the system. The conditional likelihood function for this entity is given by:

$$L_j(h_0(t_{ij})|z_j) = \left[\prod_{i=1}^{n_j} (z_j h_0(t_{ij}))^{\delta_{ij}} \right] \dots \times \exp[-z_j (H_0(\tau_j) - H_0(S_j))] \quad (8)$$

with $H_0(t)$ the cumulative hazard function given in Equation (9).

$$H_0(t) = \omega t^\rho \quad (9)$$

τ_j and S_j represent respectively the final and the starting times of the observation period for the component j . Let assume that $S_j = 0$ day as an initial time for the model.

The conditional likelihood function for this component with respect to z_j is given in the equation (10).

$$L_j(\theta|h_0(t_{ij})) = \int_0^\infty \left[\prod_{i=1}^{n_j} (z_j h_0(t_{ij}))^{\delta_{ij}} \right] \dots \times \exp(-z_j H_0(\tau_j)) f(\theta|z_j) dz_j \quad (10)$$

By replacing gamma distribution and using gamma function properties, the marginal or unconditional likelihood function for component j is

$$L_j(\omega, \rho, \theta) = \frac{\left[\prod_{i=1}^{n_j} (h_0(t_{ij}))^{\delta_{ij}} \right] \Gamma(d_j + \frac{1}{\theta}) \theta^{d_j}}{\Gamma(\frac{1}{\theta}) [\theta H_0(\tau_j) + 1]^{(d_j + \frac{1}{\theta})}} \quad (11)$$

with $d_j = \sum_{i=1}^{n_j} \delta_{ij}$.

Equation (11) was developed in this study and is of great importance as it takes into account the frailty effect, censored data and the stochastic process of repairable components, the NHPP. This increases the probability of having a model that matches the historical maintenance data and will enable vital information to be extracted. Moreover, instead of simplifying the model by considering the final time τ_j as a constant for all components as seen in the literature, we manage to keep it individual in order to model the exact effect of the heterogeneity that differentiates the components.

For m components in the system, the total likelihood function is the sum of likelihood function for each component. Therefore, the marginal likelihood function for the system is:

$$L = \sum_{j=0}^m L_j(\omega, \rho, \theta) \quad (12)$$

The simplest way to handle this complex expression is to use the logarithmic function. Therefore, the logarithm of the marginal likelihood function for m components is

$$l_{\text{marg}} = \sum_{j=1}^m \left[\sum_{i=1}^{n_j} \delta_{ij} (\log \omega + \log \rho + (\rho - 1) \log(t_{ij})) \right] \dots + \sum_{j=1}^m \left[\log \Gamma(d_j + \frac{1}{\theta}) + d_j \log(\theta) - \log \Gamma(\frac{1}{\theta}) \right] \dots - \sum_{j=1}^m \left[(d_j + \frac{1}{\theta}) \log(\theta \omega \tau_j^\rho + 1) \right] \quad (13)$$

The maximum of the marginal likelihood function is the value at which parameters (ω, ρ, θ) are optimums. Let find the partial derivative of marginal likelihood with respect to each parameter of the model. Equations (14,15,17) give these partial derivatives.

$$\frac{\partial l_{\text{marg}}}{\partial \omega} = \sum_{j=1}^m \left[\left(\sum_{i=1}^{n_j} \delta_{ij} \frac{1}{\omega} \right) \right] \dots - \sum_{j=1}^m \left[(1 + \theta d_j) \frac{\tau_j^\rho}{1 + \theta \omega \tau_j^\rho} \right] \quad (14)$$

$$\frac{\partial l_{\text{marg}}}{\partial \rho} = \sum_{j=1}^m \left[\left(\sum_{i=1}^{n_j} \delta_{ij} \left(\frac{1}{\rho} + \log(t_{ij}) \right) \right) \right] \dots - \sum_{j=1}^m \left[(1 + \theta d_j) \left(\frac{\omega \tau_j^\rho \log \tau_j}{1 + \theta \omega \tau_j^\rho} \right) \right] \quad (15)$$

Define number of iteration N
 Define number of components m
 Define the learning rate α
 Define initial values of parameters $\omega_1, \rho_1, \theta_1$
Data: Input $t_{ij}, \tau_j, \delta_{ij}, n_j$
while $k < N$ **do**
 while $j < m$ **do**
 while $i < n_j$ **do**
 compute expressions in marginal likelihood and partial derivatives function starting from $i=1$ to n_j ;
 end
 compute expressions in marginal likelihood and partial derivatives function starting from $j=1$ to m ;
end
 $l_{marg}(\omega_k, \rho_k, \theta_k)$;
 $grad_{\omega} = \frac{\partial l_{marg}}{\partial \omega}(\omega_k, \rho_k, \theta_k)$;
 $grad_{\rho} = \frac{\partial l_{marg}}{\partial \rho}(\omega_k, \rho_k, \theta_k)$;
 $grad_{\theta} = \frac{\partial l_{marg}}{\partial \theta}(\omega_k, \rho_k, \theta_k)$;
 $\omega_{k+1} = \omega_k + \alpha \times grad_{\omega}$;
 $\rho_{k+1} = \rho_k + \alpha \times grad_{\rho}$;
 $\theta_{k+1} = \theta_k + \alpha \times grad_{\theta}$
end
Result: Plot l_{marg}
Result: Print $(\omega_l, \rho_l, \theta_l)$, with l the index of maximal value of l_{marg}
 Algorithm 1: Stochastic Gradient Descent Algorithm.

The partial derivative with respect to θ is done using the property of derivative of $\log \Gamma(u)$ which involves the use of digamma function $F(u)$ such as

$$\frac{d}{du} \log \Gamma(u) = \frac{\Gamma'(u)}{\Gamma(u)} = u'F(u) \quad (16)$$

Using Equations (13) and (16), the partial derivative of the logarithm of the marginal likelihood function with respect to θ is

$$\begin{aligned} \frac{\partial l_{marg}}{\partial \theta} = & \sum_{j=1}^m \left[\frac{d_j}{\theta} - \frac{1}{\theta^2} F\left(d_j + \frac{1}{\theta}\right) + \frac{1}{\theta^2} F\left(\frac{1}{\theta}\right) \right] \dots \\ & + \sum_{j=1}^m \left[\frac{1}{\theta^2} \log(1 + \theta \omega \tau_j^{\rho}) \right] \dots \\ & - \sum_{j=1}^m \left[\left(d_j + \frac{1}{\theta}\right) \frac{\omega \tau_j^{\rho}}{1 + \theta \omega \tau_j^{\rho}} \right] \end{aligned} \quad (17)$$

In this study, we use the stochastic gradient decent (SGD) algorithm for optimizing the likelihood function, as it is a Newton-Raphson method that has given better results in the literature (Haji and Abdulazeez, 2021, Mercier et al., 2018).

Algorithm 1 gives details on the stochastic gradient descent method used for this study. We first define all functions and compute them at each step of iteration and get optimum parameters at maximum likelihood value for a specific family.

Finally, we calculate the frailty parameter z , the cumulative hazard function and the reliability function. These functions enable us to classify the risk of cracking within a family. A comparison between two turbine families is adopted to validate what has been observed: turbine runners (groups) from family B crack more than those from family A. We therefore used the same length of observations for both families.

2.3.3 Frailty Parameter

Previous research has treated z as a random variable. In this study, as we are motivated to compare the risk of cracking between individuals, we adopt another approach to derive the value of z immediately from censored data. From equation (8), we can obtain the frailty parameter that maximizes the conditional likelihood function L_j . The logarithm of the conditional likelihood function L_j for a specific component is given by equation (18).

$$\begin{aligned} \log(L_j(\omega, \rho, \theta)) = & \left[\sum_{i=1}^{n_j} \delta_{ij} (\log(z_j) + \log \omega + \log \rho) \right] \dots \\ & + \left[\sum_{i=1}^{n_j} \delta_{ij} + (\rho - 1) \log(t_{ij}) \right] - z_j \omega \tau_j^{\rho} \end{aligned} \quad (18)$$

Consequently, the optimal frailty parameter that expresses the data for the j component is obtained by calculating the partial derivative of Equation (18) with respect to z_j and equalizing it to zero. This yields

$$z_j = \frac{\sum_{i=1}^{n_j} \delta_{ij}}{\omega \tau_j^{\rho}} \quad (19)$$

Equation (19) reveals that z_j is highly dependent on the failure status data δ_{ij} and the final event time for component j . If no failure is recorded during the observation period, the value of z_j equals zero and frailty distribution can no longer be used for that specific component. However, the contribution of that component with zero frailty have been included in the overall system model in the marginal likelihood expression.

2.3.4 Reliability

With the parameters of the model and frailty effect, it is easier to compute the unconditional reliability of

the component j as given in Equation (20).

$$R_j(t|z_j) = \exp(-z_j \omega t^p) \quad (20)$$

In addition, the marginal reliability function for the same component is given by

$$R_j(t) = \int_0^\infty f(z_j; \theta) \exp(-z_j \omega t^p) dz_j \quad (21)$$

3 SIMULATIONS

3.1 Events Data

To validate the model, we choose two different families of turbine runners. Family A has reliable groups than family B. We also choose the same observation period to compare the curves of the two families. Within the same family, the frailty effect will play a role in differentiating turbine runners. This will enable comparisons to be made within and between families. The data used for simulations are the real observation times (inspections and crack repairs) and failure statuses for ten Francis turbine runners belonging to families A and B. The failure statuses provide information on censoring. The observation period runs from January 2001 to January 2022. Data are collected from the maintenance history database. Tables 1 and 2 show the age in years of the ten groups at the start of the observation period.

Table 1: Age for groups in family A (years).

GR 01	GR03	GR05	GR07	GR10
19	19.5	19.7	20	21.2

Table 2: Age for groups in family B (years).

GR 01	GR03	GR05	GR07	GR10
19.4	19.5	20	20.1	21.4

Table 3 gives the observed event times for family A, and the corresponding failure statuses are in Table 4.

In the same way, table 5 contains recorded event times data for family B and the corresponding failure statuses are in Table 6.

3.2 Results and Discussion

We use the SGD algorithm described in section 2.3.2 and the data in section 3.1. The learning rate is 0.0071 for both families. The initial parameters used for families A and B are given in Table 7.

Table 3: Event times for groups in family A (days).

GR 01	GR03	GR05	GR07	GR10
1304	1739	674	737	369
1403	3057	1373	2199	1102
1892	3427	1495	2483	2602
3427	3708	1556	3427	3393
3680	6701	2314	3708	3617
4009		2347	5036	
5593		3057		
6236		3176		
		3427		
		3708		
		4394		
		5575		

Table 4: Failure Statuses for groups in family A.

GR 01	GR03	GR05	GR07	GR10
0	0	0	0	0
1	0	0	0	1
0	0	1	0	1
0	0	0	0	0
1	0	0	0	0
0		1	0	
0		0	0	
0		0		
		0		
		0		
		1		
		0		

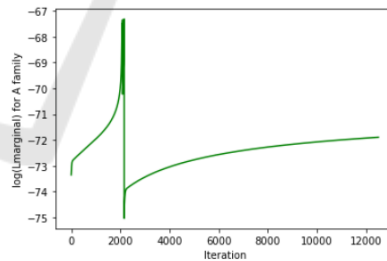


Figure 2: Evolution of the logarithm of the marginal likelihood function for family A.

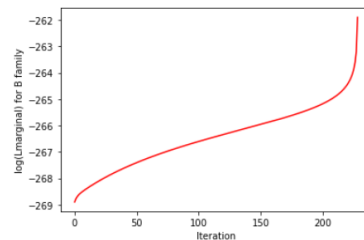


Figure 3: Evolution of the logarithm of the marginal likelihood function for family B.

Table 5: Event times for groups in family B (days).

GR 02	GR04	GR06	GR08	GR09
292	794	947	347	823
613	1283	1102	766	977
895	1495	1523	947	1495
1403	1768	2255	1130	2227
1892	2089	2497	1201	2868
2347	2588	2679	1710	3232
2658	2889	2854	2227	3624
2777	3202	3099	2595	4062
3260	3379	3253	2847	4412
3687	3533	3638	3134	4636
3722	4002	4051	3561	4715
3911	4379	4410	3981	5085
4445	4711	4051	4392	5441
4716		4755	4442	5469
5184		5195	4606	5777
5423		5406	5040	6081
5709		5816	5830	6238
			6311	6311
			6660	6531
			6733	6965
			7091	7336

Table 6: Failure statuses for groups in family B.

GR 02	GR04	GR06	GR08	GR09
1	0	0	1	0
0	0	1	1	0
0	0	0	0	0
1	0	0	1	0
0	1	0	0	0
0	1	0	0	0
0	0	0	1	0
0	0	0	0	1
1	0	0	0	0
0	0	0	0	0
1	0	0	0	1
0	1	0	0	0
1	0	1	1	0
1		1	0	1
1		0	0	0
1		1	1	1
1			1	1
			1	1
			1	0
			1	0
			0	0

After running the algorithm, Figure 2 illustrates the evolution of the logarithm of the marginal likelihood function for family A, and the corresponding optimal parameters obtained are shown in Table 8. Similarly, the algorithm run for family B groups

Table 7: Initial parameters of the model.

	ω	ρ	θ
Family A	2	0.5	3
Family B	2	1.0	3

gives the evolution of the logarithm of the likelihood function in Figure 4, and the corresponding optimal parameters are in table 9. In Figure 3, we have a single optimal value obtained before 3000 iterations, enabling us to obtain better expressed results. In family A, on the other hand, another local optimum can be obtained with more iterations.

For both families, the ω scaling parameter is almost the same. This is because we took the same observation period for both families.

However, the shape parameter ρ in family A is less than 1, which implies that the system is improving after maintenance. If we look at the failure statuses data in Table 4 for family A, we observe that no failure was recorded in two groups during the observation period: GR03 and GR07. This strongly affected the results. In fact, in family B, ρ is greater than 1, definitively confirming the reality that the system is defined as a sad system, with many cracking as indicated by the real data (Table 6). The results reveal the importance of having taken failure statuses into account in the overall model.

The optimal parameter θ demonstrates the spread of heterogeneity among turbine runners in the same family. In family B, the frailty variance θ is higher than in family A. Figure 4 shows the frailty probability density function curve for family B above that of family A. This leads to a lower frailty impact in family A than in family B.

Table 8: Optimal parameters of the model and the maximum value of the logarithm of the marginal likelihood function

	ω	ρ	θ	l_{marg}
Family A	0.011	0.56	3.77	-67
Family B	0.029	1.07	4.77	-262

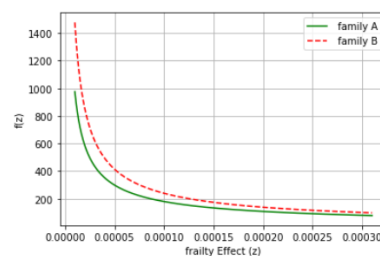


Figure 4: Gamma frailty function for families A and B.

Let use Equation (19) that gives the expression of z_j and get values of frailty effect as given in Tables 9 and 10 for families A and B respectively .

Table 9: Frailty effect z for family A.

GR01	GR03	GR05	GR07	GR10
1.35	0.0	2.15	0.0	1.82

Table 9 highlights that GR03 and GR07 have no frailty effect. These two groups cannot therefore be modeled using the frailty effect. We use only the NHPP with the power law to model them. Among the groups in this family with non-zero z values, GR01 has the lowest value. Consequently, a lower value of heterogeneity would be associated with higher reliability.

Table 10: Frailty effect z for family B.

GR02	GR04	GR06	GR08	GR09
0.029	0.012	0.013	0.026	0.015

Likewise, in Table 10, GR02 has the lowest fragility z -value and should be the most reliable in family B.

Using equation (9), we can obtain the cumulative hazard function for GR03 and GR07 as they have no frailty. For these groups with a non-zero frailty effect, Equation (9) must be multiplied by the corresponding z_j as in Equation (3). Figures 5 and 6 illustrate the cumulative hazard function for families A and B respectively. In family A, GR05 is the most vulnerable, representing the highest risk of cracking damage. GR03 and GR07, on the other hand, have no frailty effect and are considered as homogeneous and more reliable, as shown in Figure 7. Their two curves do not allow to conclude whether they have the same risk of cracking or not. We can notice that they almost stick together.

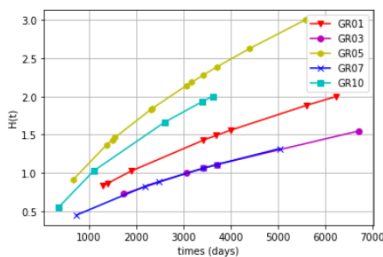


Figure 5: Cumulative Hazard function for family A.

In Figure 6, we can notice that all groups start with the same low risk of cracking. As time goes on, the curves become more scattered and confirm the Table 8. However, the cumulative hazard function curves

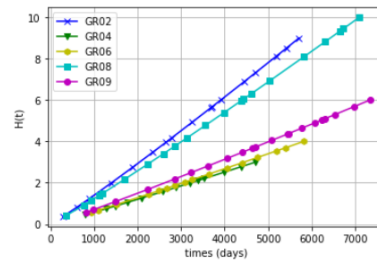


Figure 6: Cumulative Hazard function for family B.

of the two groups (GR04 and GR06) stuck together. They represent the same risk of cracking. In the same Figure 6, curves of groups GR09, GR04 and GR06 are going in the same direction. So, instead of wasting inspection time on both, see Table 6, the maintenance team could decide to monitor only one of the two and apply the same decisions obtained on the other, considering them as twin turbine runners. In the same way, the GR02 and GR08 curves are close to each other. An examination of the data on failure statuses reveals that, at the end of their operating life, they recorded multiple successive cracks.

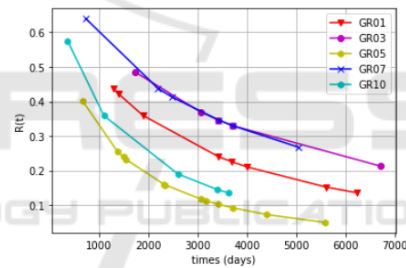


Figure 7: Conditional reliability for A family.

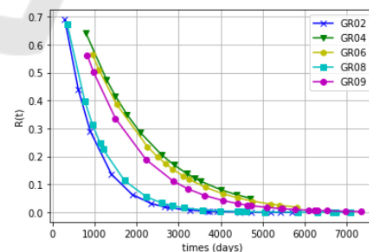


Figure 8: Conditional reliability for B family.

Figures 7 and 8 have been plotted using equation (20). They illustrate the reliability for families A and B respectively. For the same period, 3000 days for example, all groups in family B have a reliability below 20%, whereas in family A, we have three groups (GR01, GR03 and GR07) with a reliability above 20%. This confirms that these three groups are the most robust. The duration of systematic inspections

could be much longer for them. Furthermore, in Figure 8, after 5,000 days, it appears that all the groups have collapsed. These groups have been replaced or modified supporting the model.

4 CONCLUSIONS

The study is based on a comparison of the reliability of ten turbines belonging to two different families, using a frailty model. To do this, we used a non-homogeneous Poisson process with a power law and the gamma frailty distribution. The model parameters are found by optimizing the marginal likelihood function developed in the study. The likelihood function takes into account censored historical maintenance data, the gamma frailty distribution and the final individual observation time. In addition, the frailty effect z is not considered as a random variable, but is derived directly from the optimization of the individual conditional likelihood function. However, for turbine runners with no observed failures, the heterogeneity effect was zero, which led us to abandon the frailty model in this case. We have discovered that by deriving z , the frailty effect, as an expression of failure statuses and individual final observation time, and adding censoring to the model, the reliability curves express the results much better and are very close to reality. For example, groups in family B that have been replaced due to recurring cracks have a reliability of less than 20% at 3,000 days and have collapsed at around 5,000 days, whereas groups in family A are robust. Despite the fact that we neglected covariates in the model, we obtained informative results that may help the maintenance team to group turbines with the same reliability trend and monitor only one turbine in order to reduce double inspections. This study could be strengthened by adding important covariates such as age, turbine runner modification, start-up and shutdown frequencies. Future work could also focus on optimizing systematic inspections with regard to the evolution of reliability curves, and avoiding the multiplication of maintenance shutdowns, which have a negative impact on cracking.

ACKNOWLEDGEMENTS

The authors are grateful to *Turbomachinery Laboratory of the Engineering School of the University of Quebec in Abitibi-Témiscamingue (UQAT)*, to *Hydro-Québec's Research Institute* and to *Hydro-Québec* for the collaboration.

REFERENCES

- Abbring, J. H. and Berg, G. J. V. D. (2007). The unobserved heterogeneity distribution in duration analysis. In *Biometrika*. 94(1).
- Ascher, H. E. (1968). Evaluation of repairable system reliability using the bad-as-old concept. In *IEEE Transactions on Reliability*. 17(2).
- Ascher, H. E. (2008). Repairable systems reliability. In *Encyclopedia of Statistics in Quality and Reliability*. 1.
- Asfaw, Z. G. and Lindqvist, B. H. (2015). Unobserved heterogeneity in the power law nonhomogeneous poisson process. In *Reliability Engineering and System Safety*. 134.
- Bajgholi, M. E., Rousseau, G., Viens, M., and Thibault, D. (2021). Capability of advanced ultrasonic inspection technologies for hydraulic turbine runners. In *Applied Sciences*. 11.
- Bajgholi, M. E., Rousseau, G., Viens, M., Thibault, D., and Gagnon, M. (2023). Reliability assessment of non-destructive testing (ndt) for the inspection of weld joints in the hydroelectric turbine industry. In *The International Journal of Advanced Manufacturing Technology*. 128.
- Brown, B., Liu, B., McIntyre, S., and Revie, M. (2023). Reliability evaluation of repairable systems considering component heterogeneity using frailty model. In *Proceedings of the Institution of Mechanical Engineers, Part O: Journal of Risk and Reliability*. 237(4).
- Duchateau, L. and Janssen, P. (2008). The frailty model. In *New York: Springer Verlag*. 1.
- Gagnon, M. and Nicolle, J. (2019). On variations in turbine runner dynamic behaviours observed within a given facility. In *Conference Series: Earth and Environmental Science*. 450(1).
- Gagnon, M., Tahan, A., Bocher, P., and Thibault, D. (2014). Influence of load spectrum assumptions on the expected reliability of hydroelectric turbines: A case study. In *Structural Safety*. 50.
- Gagnon, M., Tahan, S. A., Bocher, P., and Thibault, D. (2010). Impact of startup scheme on francis runner life expectancy. In *25th IAHR Symposium*. Timisoara.
- Georgievskaja, E. (2020). Predictive analytics as a way to smart maintenance of hydraulic turbines. In *Procedia Structural Integrity*. 28.
- Georgievskaja, E. (2021). Analytical system for predicting cracks in hydraulic turbines. In *Engineering Failure Analysis*. 127.
- Haji, S. H. and Abdulazeez, A. M. (2021). Comparison of optimization techniques based on gradient descent algorithm: A review. In *PalArch's Journal of Archaeology of Egyptology*. 18(4).
- Hydro-Québec (2023). Annual report. In *Report*. 1.
- Ivanchenko, I. P. and Prokopenko, A. N. (2020). Analyzing the operational materials on crack formation in blades of francis turbines at the krasnoyarsk hpp. In *Power Technology and Engineering*. 53(6).

- Liu, X., Luo, Y., and Wang, Z. (2016a). A review on fatigue damage mechanism in hydro turbines. In *Renewable and Sustainable Energy Reviews*. 54.
- Liu, X., Luo, Y., and Wang, Z. (2016b). A review on fatigue damage mechanism in hydro turbines. In *Renewable and Sustainable Energy Reviews*. 54.
- Love, C. E. and Guo, R. (1991). Application of weibull proportional hazards modelling to bad-as-old failure data. In *Quality and reliability engineering international*. 7(3).
- Morin, O., Thibault, D., and Gagnon, M. (21-26 March 2021). the comparison of hydroelectric runner fatigue failure risk based on site measurements. In *30th IAHR Symposium on Hydraulic Machinery and Systems*. Lausanne.
- Munda, M., Rotolo, F., and Legrand, C. (2012). parfm: Parametric frailty models in r. In *Journal of Statistical Software*. 51.
- Oliveira, M. D. D., Colosimo, E. A., and Gilardoni, G. L. (2013). Power law selection model for repairable systems. In *Communications in Statistics-Theory and Methods*. 42(4).
- Slimacek, V. and Lindqvist, B. H. (2016). Nonhomogeneous poisson process with nonparametric frailty. In *Reliability Engineering and System Safety*. 149.
- Therneau, T. M., Grambsch, P. M., and Pankratz, V. S. (2003). Penalized survival models and frailty. In *Journal of computational and graphical statistics*. 12(1).
- Thibault, D., Gagnon, M., and Godin, S. (2015). The effect of materials properties on the reliability of hydraulic turbine runners. In *International Journal of Fluid Machinery and Systems*. 8.
- Trivedi, C. and Cervantes, M. (2017). *Fluid-structure interactions in Francis turbines : A perspective review*. Renewable and Sustainable Energy Reviews, 68, 87-101 edition.
- Trivedi, C., Gandhi, B., and Cervantes, M. (2013). Effect of transients on francis turbine runner life: a review. In *Journal of Hydraulic Research*. 51(2).
- Vaupel, J. W., Manton, K. G., and Stallard, E. (2023). The impact of heterogeneity in individual frailty on the dynamics of mortality. In *Demography*. 16(3).
- Wang, X. F., Li, H. L., and Zhu, F. (2012). The calculation of fluid-structure interaction and fatigue analysis for francis turbine runner. In *IOP conference series: earth and environmental science*. 15-5.
- Wienke, A. (2010). Frailty models in survival analysis. In *Chapman and Hall/CRC*. 1.
- Xiao, R., Wang, Z., and Luo, Y. (2008). Dynamic stresses in a francis turbine runner based on fluid-structure interaction analysis. In *Tsinghua Science and Technology*. 13(5).
- Xiao, R., Wang, Z., and Luo, Y. (2010). Effect of welding technologies on decreasing welding residual stress of francis turbine runner. In *Journal of Materials Science and Technology*. 26(10).
- Zhang, Y., Zheng, X., Li, J., and Du, X. (2019). Experimental study on the vibrational performance and its physical origins of a prototype reversible pump turbine in the pumped hydro energy storage power station. In *Renewable energy*. 130.